Those with small deletions (patient 14) were expected to have two green and one red signal. FISH signals were counted in 205~457 nuclei of the 4 patients (including the control patient). Although six cells were obtained from patient 12, metaphase FISH was unsuccessful because of the scarcity of metaphase cells on FISH slides.

Results

Chromosome analyses

Patient data and karyotypes are summarized in Table 1. In nine patients (six MDS cases, one MPN case, one AML case, and one case of NHL in a leukemic phase), the del(20q) was the sole abnormality. Two of the five AML patients had trisomy 8, another had trisomy 1q and monosomy 7q due to a t(1;7), and one other had trisomy 1q and monosomy 16q due to a t(1;16), all in addition to the del(20q). Although the del(20q) clone was predominant in the metaphase cells of patient 12, who had WM and a B-cell–lineage malignancy, 1 of 24 cells showed a del(7q) and a normal pair of chromosomes 20 in the TPA-stimulated culture. At that time, the cell was not recognized as a clone; as the only del(7q) cell, it did not meet the criteria for a clone (12). Patient 15, who carried an inv(16) aberration at the initial stage and served as a control for FISH, was in remission and had only normal karyotypes.

Most of 20q was lost in eight cases (large deletions in patients 2, 3, 5, 7, 9, 11, 12, and 13), and one positive Q-band (q12 or q13.2) remained in six cases (small deletions in the remaining patients). However, accurate delineation was impossible using the banding technique (Table 1).

Microarray CGH analyses

We used aCGH to accurately define the breakpoints and CDR in the del(20q) cases. Figures 1 and 2 and Table 2 show the positive aCGH results of 12 patients. All of the deletions were interstitial, and both the proximal and distal breakpoints varied among patients. The centromeric breakpoints were located in the 20q11.21~12 region, and the telomeric breakpoints in the 20q13.13~13.33 region. The extent of the deletion ranged from 11.2 to 27.3 Mb. The deletion was recognized microscopically as "large" when it was greater than 18 Mb and "small" when it was less than 15 Mb. However, two patients displayed an intermediate deletion (patients 4 and 9), suggesting that the two categories provide inadequate definition in such cases. The commonly deleted region was defined as chr20:39,933,662–47,180,979, and the deletion's size was estimated to be 7.2 Mb (Table 2 and Figure 2), corresponding to chromosome bands 20q12~20q13.13. Two commonly retained regions (CRRs) were present. The one located proximal to 30,100,973 bp corresponds to chromosome bands 20q11.1~20q11.21 and is 3 Mb in length. The other is a subtelomeric CRR distal to 58,444,848 bp within band 20q13.33 and is 4 Mb in length (Table 2 and Figure 2).

Patients who demonstrated multiple clones in the chromosome analysis showed some inconsistent results regarding clone size between the karyotype and aCGH analyses. Patient 12 displayed 25 del(20q) cells (89.2%) and 3 normal cells in the overnight culture without any stimulation (Table 1). The aCGH analysis of the DNA sample from this culture revealed a predominant del(7q) clone and a del(20q) clone that was less frequent (data not shown). The del(7q) clone was detected in only one metaphase cell from the

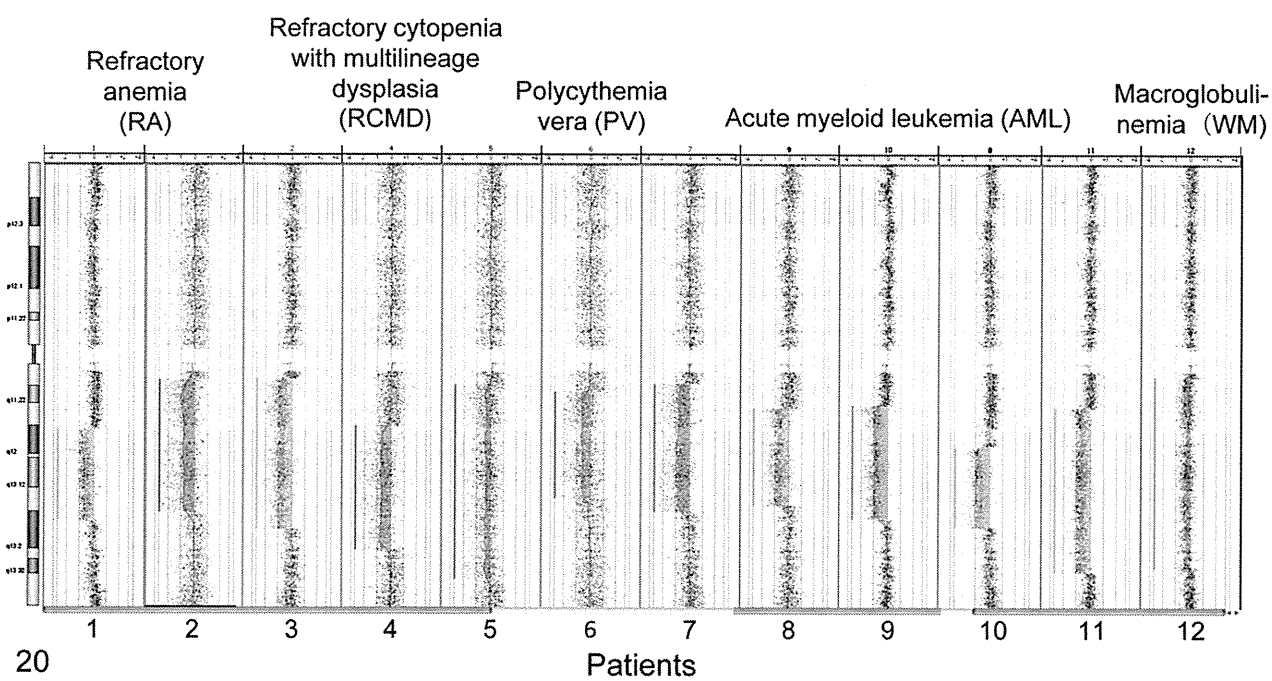

Figure 1 The results of aCGH analyses of del(20q). Patients 1–2, RA; 3–5, RCMD; 6, PV; 7–11, AML; 12, WM. Left shifts indicate the deleted segments of 20q. A slight shift was observed in two patients (patients 5 and 12), reflecting the coexistence of normal and abnormal clones in the samples.

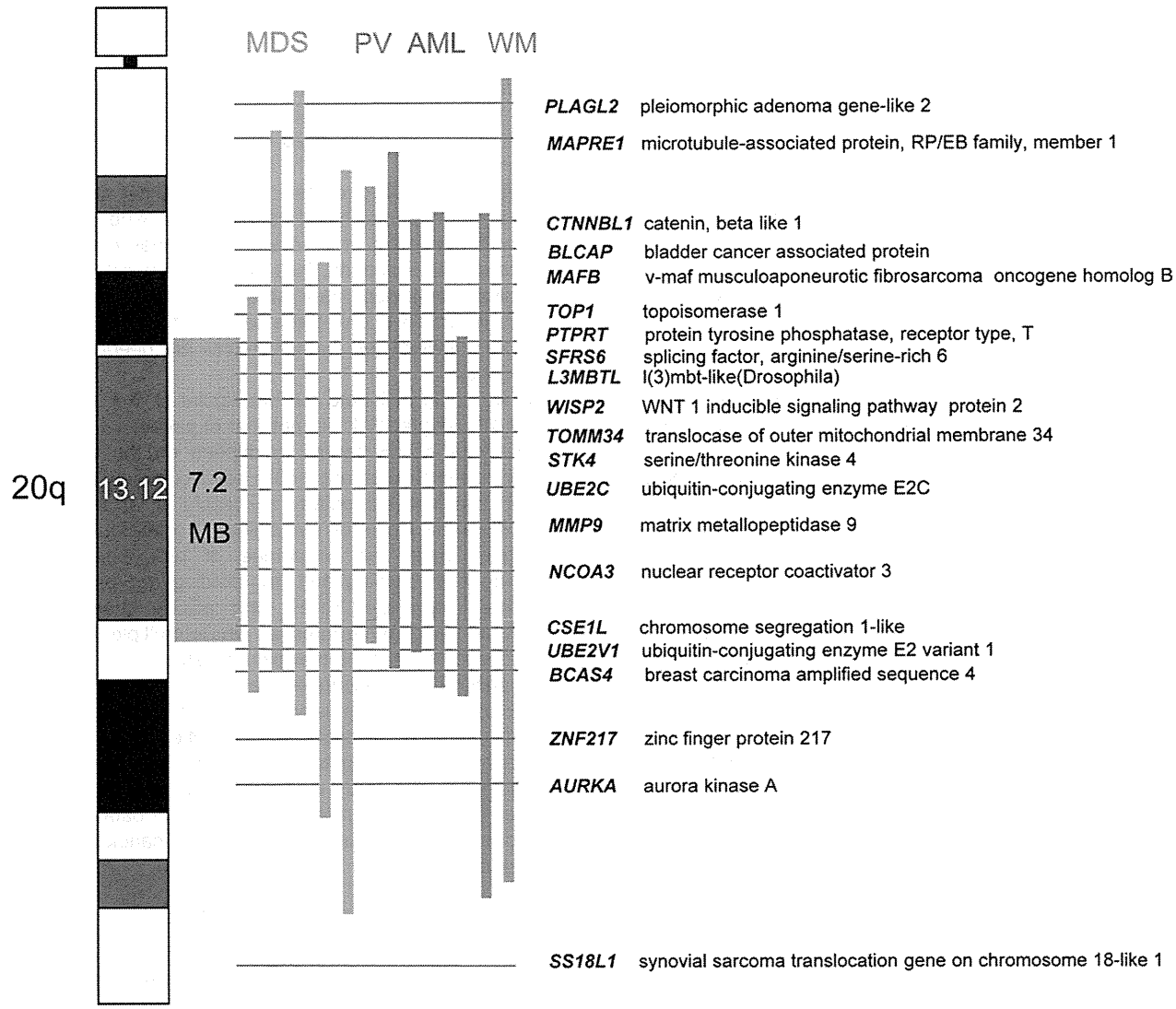

Figure 2 An ideogram of the long arm of chromosome 20. The 12 colored bars indicate the deleted regions in each patient. The bars are arranged in order of the patients' number, from patient 1 (left) to patient 12 (right). The CDR is shown by the gray rectangle. Some of the genes mapped within and around the region are listed; these genes relate to cell cycle regulation, apoptosis, transcription, or tumor development and progression based on the Human March 2006 Assembly (NCBI build 36.1, hg18).

TPA-stimulated 7-day culture (Table 1). Furthermore, the del(20q) was not detected in the aCGH analyses in patients 13 and 14, although they demonstrated a del(20q) clone in 14 of 29 (48.3%) and 9 of 26 (34.6%) of their metaphase cells, respectively (Table 1).

FISH results

The results of FISH analyses are shown in Table 3. Dual-color FISH demonstrated that del(20q) cells lost both 20q probes in patients 12 and 13, showing a large deletion. This resulted in one green and one red signal in del(20q) cells, as expected. The del(20q) cells of patient 14 demonstrated two FITC-labeled probe signals. The cells showed a pattern with two green and one red signal, corresponding to a small deletion, del(20)(q12q13.3), observed on karyotype analysis.

The frequency of del(20q) cells detected with interphase FISH was lower than that of del(20q) metaphase cells detected using karyotype analyses in the three patients. In the first karyotype analyses, the del(20q) chromosomes were detected in 89.2%, 48.2%, and 34.6% of cells in patients 12, 13, and 14, respectively, and in 80.0%, 30.0%, and 23.5% in the additional examination after a long period of cell storage (Tables 1 and 3). In the FISH experiments, the del(20q) was detected only in 22.4%, 12.9%, and 11.7% of interphase nuclei of the three patients, respectively.

Discussion

We delineated the accurate breakpoints of del(20q) chromosomes using an aCGH technique. The results show that the

deletions vary between 11.2 and 27.3 Mb rather than being classifiable into two distinct categories, large and small. The 7.2 Mb CDR ranges from the distal region of 20q12 to the proximal region of 20q13.13, the center of which contains 20q13.12 (Figure 2). The CDR of our study is more distal than any reported previously, which have ranged from 20q11.2 to 20q12~13.12 (5–7,13,14). Recently, Huh et al. (8) characterized two CDRs and two CRRs on 20q using a genomewide single nucleotide polymorphism array. They reported that CDR1 spanned 2.5 Mb between bands 20q11.23 and 20q12, whereas CDR2 encompassed 1.8 Mb within 20q13.12, CRR1 spanned 1.9 Mb within 20q11.21, and CRR2 encompassed 2.5 Mb within 20q13.33. Comparing our data with those of Huh et al. (8), our CDR (39,933,662–47,180,979 bp) does not include CDR1 (34,968,632–37,417,814 bp), and is located more distally than their regions. These differences might be partly due to the techniques used. Further studies with a larger number of patients would resolve this issue.

It has been suggested that one or more tumor suppressor genes could be located in the CDR, the deletion or inactivation of which may play a role in malignant growth (3,7,14–18). Among the genes within the CDR, *L3MBTL1* was recently reported to be a candidate tumor suppressor gene, with a proposal that the loss of the L3MBTL 1 protein contributed to the development of 20q– hematopoietic malignancies by inducing genomic instability (18). However, as so many genes lie within and around the region, it is possible that multiple genes are involved in malignant development. Genes located in the retained chromosomal regions may also be important in tumor pathogenesis, as pointed out by Douet-Guilbert et al. (7). Some of the genes relating to cell cycle regulation, apoptosis, transcription, or tumor development and progression in these regions are shown in Figure 2 based on the Human March 2006 Assembly (NCBI build 36.1, hg18). To find mutations in the candidate genes present in the CDR or CRR, studies with next-generation sequencing techniques coupled with a target enrichment system (Agilent Technologies) are now in progress, using several of the present patients. If no mutation is found, the hypothesis of haploinsufficiency of multiple genes on 20q might be considered, as supported by Huh et al. (8).

A difference in the techniques used produced some inconsistent results in clone size for patients 12, 13, and 14. Patient 12 was diagnosed with WM and showed frequent del(20q) cells in his karyotype analyses. Del(20q) is rarely reported in cases of lymphoid malignancies (2). Our aCGH analysis suggested that most cells of this patient carried a del(7q) abnormality (data not shown). We considered the possibility that the del(20q) clone comprised not lymphoid cells, but MDS cells, which demonstrated a growth advantage in vitro. However, bone marrow smears revealed that more than 90% of the cells were tumor cells, and no characteristics of MDS were found. Thus, we assumed that the del(20q) cells were lymphoid cells, although their pathogenic role was unclear. A del(20q) was not detected by aCGH in patient 13 or 14, in whom more than 30% of metaphase cells demonstrated the deletion in the first karyotype analysis (Tables 1 and 2). FISH analyses were performed to estimate the clone size of del(20q) cells in patients 12, 13, and 14 (Table 3). The frequency of del(20q) cells detected by interphase FISH was 22.4% in patient 12, 12.9% in patient 13, and 11.7% in patient 14. The results show that del(20q) cells were detected at a higher frequency in metaphase cells by karyotype analyses than in interphase nuclei using FISH. In addition, FISH patterns of del(20q) were more frequently observed in big nuclei, which were thought to be in a dividing stage, than in small, compact nuclei in a resting stage. To explain this, a few possibilities may be considered: del(20q) cells might have a growth advantage in vitro; normal lymphocytes might decrease the frequency of del(20q) because of peripheral blood contamination when the bone marrow is aspirated; or a selection bias may occur in the microscopic observations. It is possible that cell dynamics and mitotic behaviors vary among patients, and as our results are limited to only three patients, two of whom have lymphoid malignancies, further studies are needed to draw a conclusion.

As we could delineate the breakpoint of the del(20q) of patient 12 using aCGH, but not that of patient 13 or 14, the sensitivity of aCGH seems to depend on the target cell density. It is likely that target cells need to occupy more than 20% of the cell population for a successful aCGH analysis, at least within the limits for our cases. The aCGH and FISH techniques have the advantage of producing findings regarding both dividing and non-dividing cell populations. Therefore, karyotype, FISH, and aCGH analyses can complement each other in cases where multiple clones are present, such as in bone marrow aspirates.

In conclusion, we accurately delineated the breakpoints of a del(20q) in 12 patients using an aCGH analysis, which has the advantage of detecting abnormalities in non-dividing cells, although this is limited to copy number changes. The CDR found in our study is located more distally than any reported previously. Further accumulation of data is needed to resolve this discrepancy and to identify candidate pathogenic genes.

Acknowledgments

This research was supported in part by Shiseikai Corporate Juridical Person.

References

1. Greenberg P, Cox C, LeBeau MM, et al. International scoring system for evaluating prognosis in myelodysplastic syndromes. Blood 1997;89:2079–2088.
2. Mitelman F. Catalog of chromosome aberrations in cancer. New York: Wiley-Liss; 1991.
3. White NJ, Nacheva E, Asimakopoulos FA, et al. Deletion of chromosome 20q in myelodysplasia can occur in a multipotent precursor of both myeloid cells and B cells. Blood 1994;83: 2809–2816.
4. Hollings PE, Rasman I, Beard ME. A 20q deletion originating in a pluripotent stem cell. Blood 1994;83:305–306.
5. Nacheva E, Holloway T, Carter N, et al. Characterization of 20q deletions in patients with myeloproliferative disorders or myelodysplastic syndromes. Cancer Genet Cytogenet 1995;80:87–94.
6. Bench AJ, Nacheva EP, Hood TL, et al. Chromosome 20 deletions in myeloid malignancies: reduction of the common deleted region, generation of a PAC/BAC contig and identification of candidate genes. Oncogene 2000;19:3902–3913.
7. Douet-Guilbert N, Basinko A, Morel F, et al. Chromosome 20 deletions in myelodysplastic syndromes and Philadelphia-chromosome-negative myeloproliferative disorders:

characterization by molecular cytogenetics of commonly deleted and retained regions. Ann Hematol 2008;87:537–544.
8. Huh J, Tiu RV, Gondek LP, et al. Characterization of chromosome arm 20q abnormalities in myeloid malignancies using genome-wide single nucleotide polymorphism array analysis. Genes, Chromosomes & Cancer 2010;49:390–399.
9. Okada M, Hirai M, Suto Y, et al. Microarray CGH analyses of hematopoietic malignancies with chromosome 20q deletions. Advances in Chromosome Science 2009;3:164–166.
10. Vardiman JW, Thiele J, Arber DA, et al. The 2008 revision of the World Health Organization (WHO) classification of myeloid neoplasms and acute leukemia: rationale and important changes. Blood 2009;114:937–951.
11. Swerdlow SH, Campo E, Harris NL, et al. WHO classification of tumours of haematopoietic and lymphoid tissues. 4th edition. Lyon, France: IARC Press; 2008.
12. Shaffer LG, Slovak ML, Campbell LJ, editors. ISCN 2009: an international system for human cytogenetic nomenclature. Basel, Switzerland: Karger; 2009.
13. Asimakopoulos FA, White NJ, Nacheva E, et al. Molecular analysis of chromosome 20q deletions associated with myeloproliferative disorders and myelodysplastic syndromes. Blood 1994;84:3086–3094.
14. Wang PW, Eisenbart JD, Espinosa R III, et al. Refinement of the smallest commonly deleted segment of chromosome 20 in malignant myeloid diseases and development of a PAC-based physical and transcription map. Genomics 2000;67:28–39.
15. Roulston D, Espinosa R III, Stoffel M, et al. Molecular genetics of myeloid leukemia: identification of the commonly deleted segment of chromosome 20. Blood 1993;82:3424–3429.
16. Asimakopoulos FA, Gilbert JGR, Aldred MA, et al. Interstitial deletion constitutes the major mechanism for loss of heterozygosity on chromosome 20q in polycythemia vera. Blood 1996; 88:2690–2698.
17. Li J, Bench AJ, Vassiliou GS, et al. Imprinting of the human L3MBTL gene, a polycomb family member located in a region of chromosome 20 deleted in human myeloid malignancies. Proc Natl Acad Sci USA 2004;101:7341–7346.
18. Gurvich N, Perna F, Farina A, et al. L3MBTL 1 polycomb protein, a candidate tumor suppressor in del(20q12) myeloid disorders, is essential for genome stability. Proc Natl Acad Sci USA 2010; 107:22552–22557.

Leukemia Research 35 (2011) 1219–1225

Contents lists available at ScienceDirect

Leukemia Research

journal homepage: www.elsevier.com/locate/leukres

Inhibition of PRAME expression causes cell cycle arrest and apoptosis in leukemic cells

Norina Tanaka[a], Yan-Hua Wang[a,*], Masayuki Shiseki[a], Minoko Takanashi[b], Toshiko Motoji[a]

[a] Department of Hematology, Tokyo Women's Medical University, Tokyo, Japan
[b] Blood Preparation Department, Japanese Red Cross Tokyo Metropolitan Blood Center, Tokyo, Japan

ARTICLE INFO

Article history:
Received 14 November 2010
Received in revised form 29 March 2011
Accepted 7 April 2011
Available online 7 May 2011

Keywords:
PRAME
siRNA
Acute leukemia
Cell cycle
Apoptosis
Differentiation

ABSTRACT

The preferentially expressed antigen of melanoma (PRAME) is known as a tumor-associated antigen, but its function in leukemia remains unclear. We investigated the function with small interfering RNA (siRNA)-induced knockdown of PRAME in a K562 cell line. After PRAME siRNA transfection, proliferation was suppressed and cell cycle analysis showed G_0/G_1 arrest, followed by apoptosis. PRAME siRNA-treated cells also showed changes in the genes affecting erythroid differentiation. We examined the *PRAME* expression levels and the S phase population of 32 acute leukemia patients at the time of diagnosis and relapse. An increase of the S phase population was accompanied by an increase of *PRAME* expression at relapse. Our results suggest that PRAME plays an important role in disease progression in acute leukemia.

1. Introduction

The preferentially expressed antigen of melanoma (PRAME) was originally described as a tumor-associated antigen recognized by autologous cytotoxic T cells against a melanoma surface antigen [1,2]. While PRAME is only expressed at a low level in a few normal tissues (testis, adrenals, ovaries and endometrium), it is over-expressed in a wide variety of malignancies, such as ovarian cancer, breast carcinoma, lung carcinomas, neuroblastoma, and various acute and chronic hematological malignancies. It has been reported that PRAME expression correlates with poor clinical outcome in breast cancer and advanced-stage neuroblastoma [3–5]. The frequency of PRAME expression was reported to be about 30–64% in acute myelogenous leukemia (AML), 22–60% in chronic myeloid leukemia (CML) and 17–42% in acute lymphoblastic leukemia (ALL) [1,6,7]. It has also been described that CML from its chronic phase to blastic crisis is characterized by an increased expression of PRAME, using microarray analysis [8,9]. In leukemia, PRAME was reported to be a useful parameter for monitoring minimal residual disease in pediatric AML [10].

As for the function of PRAME, Epping et al. showed that it seems to act as a dominant repressor of retinoic acid receptor (RAR) signaling [11]. The forced over-expression of PRAME blocked RAR-mediated differentiation, inducing growth arrest and apoptosis in the presence of the RAR ligand all-*trans* retinoic acid in solid tumor cell line models. Recently, it was reported that PRAME inhibits myeloid differentiation in normal hematopoietic and leukemic progenitor cells [12]. On the contrary, Tajeddine et al. showed that PRAME induces caspase-independent cell death in leukemic cell lines and reduces tumorigenicity in vivo [13]. Thus, the function of PRAME in leukemic cells seems to be controversial.

In the present study, we investigated the function of PRAME in leukemic cells by the method of small interfering RNA (siRNA) induced knockdown of PRAME using a K562 cell line in the absence of retinoic acid (RA). K562 cells are RA-resistant, with a significantly lower number of RARs than RA-sensitive HL-60 cells [14]. After PRAME siRNA transfection, possible changes in various gene expressions were analyzed with quantitative real-time RT-PCR. In particular, the effect on cell growth, apoptosis and differentiation by suppression of PRAME expression was studied. To elucidate the clinical significance of *PRAME* expression in acute leukemia, especially its role at relapse, *PRAME* expression was examined in acute leukemia at the time of diagnosis and at relapse in paired samples. Furthermore, its relevance for the S phase population in these leukemic samples was analyzed.

2. Materials and methods

2.1. Cell culture, siRNA transfection and colony formation assays

The K562 cell line (ATCC, Manassas, VA), established from CML in blastic crisis, was used in siRNA knockdown experiments as it expressed a significant amount

* Corresponding author. Tel.: +81 3 3353 8111x31544; fax: +81 3 5269 7329.
E-mail address: yhwang@dh.twmu.ac.jp (Y.-H. Wang).

0145-2126/$ – see front matter © 2011 Elsevier Ltd. All rights reserved.
doi:10.1016/j.leukres.2011.04.005

of PRAME. The cells were cultured at 37 °C in a 5% CO_2 humidified atmosphere, in RPMI1640 medium (Invitrogen Life Technologies, Carlsbad, CA) supplemented with 10% fetal calf serum (FCS; Life Technologies, Grand Island, NY). For transfection of siRNA, 1.5×10^6 K562 cells were electroporated in an Amaxa Nucleofector I, using the Amaxa cell optimization kit V (Amaxa, Gaithersburg, MD) according to their guidelines, and then cultured on plates in three wells for each sample. An amount of 1.5 μM siRNA was used for each transfection, and the transfection efficiency and viability were analyzed after 24 h by flow cytometry, using the fluorescent expression plasmid (pmaxGFP) included in the kit. The siRNA used for PRAME knockdown was Silencer Pre-designed siRNA (Applied Biosystems, Foster City, CA; cat. no. AM16706, ID 135628). The control cells were electroporated with or without the control siRNA (Applied Biosystems). All transfections of siRNA were performed in triplicate in three independent experiments. During the suspension culture, viable cells were counted from day 1 to day 6. Cells were collected for flow cytometry, mRNA analysis and protein expression with this time course. At day 3, the cells were replated at the original cell density. Morphologic analyses of cells were performed on cytospin preparations.

Colony formation assays were performed at 24 h after transfection according to the method previously described [15]. Briefly, 2.5×10^3 transfected cells/well were seeded in microwell plates with 0.8% methylcellulose and 20% FCS. The number of colonies (>20 cells) was counted at day 7 after plating.

2.2. Cell cycle analysis

At each of day 1 to day 3 after transfection, cell cycle analysis of PRAME siRNA and control siRNA-treated cells was performed. Cells were fixed in cold ethanol and the fluorescence intensity was analyzed using a flow cytometer (EPICS-XL System II, Beckman Coulter, Miami, FL), and then the cellular DNA content distribution was analyzed with the MultiCycle for Windows (WinCycle) software program, as previously described [16].

2.3. Annexin V assay

Quantitative determination of early and late apoptotic cells was carried out using the Annexin V-FITC/Propidium iodide (PI) binding technique with the Annexin V-FITC apoptosis detection kit (Beckman Coulter), as previously described [17].

Benzyloxycarbonyl-Val-Ala-Asp fluoromethyl ketone (z-VAD-fmk) (MBL, Nagoya, Japan) or benzyloxycarbonyl-Asp-Glu-Val-Asp fluoromethyl ketone (z-DEVD-fmk) (MBL) was added to the final concentration of 100 μM to the siRNA transfected cells at 6 h after transfection and at day 3 when the cells were replated.

2.4. Caspase-3 activity assay

Cells were washed with PBS and fixed in 100% cold methanol, every 24 h from day 1 to day 6, after siRNA transfection. After incubating with an antibody against cleaved caspase-3, conjugated with Alexa Flour 488 (Beckman Coulter), positive cells were counted and analyzed as a percentage, according to the manufacturer's protocol.

2.5. Quantitative real-time reverse transcriptase-polymerase chain reaction (qRT-PCR)

Total RNA extraction, cDNA synthesis and quantitative real-time RT-PCR were performed as previously described [16] with modifications. *PRAME* expression was analyzed by the TaqMan probe method using an ABI 7500 real-time PCR system (Applied Biosystems) with co-amplification of the endogenous control gene, human *GAPDH* (Applied Biosystems). Expression levels were obtained using the standard curve method in each experiment, after normalization with the *GAPDH* gene for each sample in duplicate wells. The human *PRAME* primer–probe sets were from Applied Biosystems (assay ID: Hs00196132_m1).

The gene expression changes after siRNA transfection were surveyed using Applied Biosystems Custom TaqMan Gene Array Plates with the standard protocol. Primers and probes for 28 genes related to apoptosis, cell cycle and differentiation were set up in duplicate wells. The relative expression of each mRNA was determined by the comparative CT method using *GAPDH* expression for normalization. Changes in mRNA expression at day 1, day 3 and day 6 were recorded as the average ratio of PRAME siRNA-treated cells relative to the corresponding control siRNA cells in K562. The genes which were significantly up or down regulated in PRAME siRNA-treated cells were chosen for further analysis of their corresponding proteins.

2.6. Western blot analysis

Whole-cell lysates from K562 cells were prepared and 20 μg of protein was separated as previously described [17]. After blocking with Tris-buffered saline/0.05% Tween 20 containing 5% skim milk or 3% bovine serum albumin (Sigma, St. Louis, MO), blots were incubated at 4 °C overnight with the primary rabbit polyclonal or monoclonal antibodies against human PRAME protein (1:500 dilution; Abcam, Cambridge, UK; cat no. 32185), p27 (1:500), GATA-1, GATA-2 (1:1000; Abcam), PU.1, cleaved caspase-3 and caspase-3 (1:2000; Cell Signaling Technology, Danvers, MA), respectively. To control for equal loading, membranes were incubated with anti

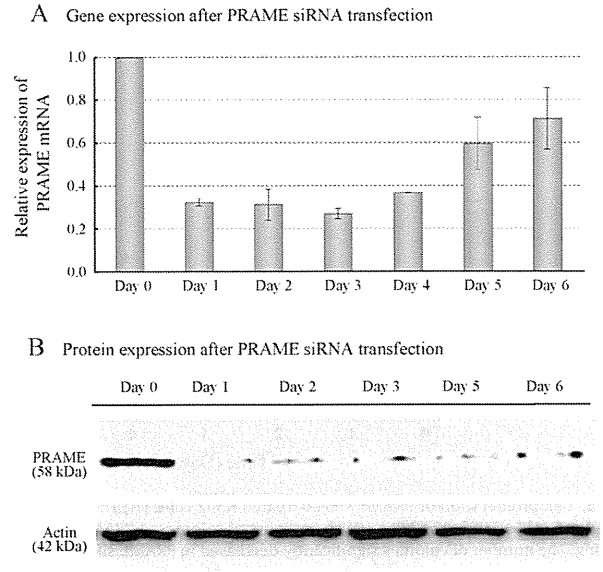

Fig. 1. (A) Changes in *PRAME* expression as the average ratio of PRAME siRNA-treated cells relative to the corresponding control cells. PRAME siRNA knockdown resulted in a reduction of *PRAME* mRNA expression of >70% from day 1 to day 3. (B) Expression of protein after PRAME siRNA transfection. The upper lane indicates that the expression of PRAME protein was inhibited almost completely from day 1 to day 6.

Actin antibody (1:1000; Sigma). As a secondary antibody, a horseradish peroxidase-conjugated anti rabbit IgG was used as recommended by the manufacturer (Sigma). The bound antibody was detected by chemiluminescence using Immobilon Western reagents (Millipore, Billerica, MA).

2.7. Patient samples

Expression of PRAME and cell cycle profiles were measured in paired samples of acute leukemia. A total of 32 (18 AML, 14 ALL) acute leukemia patients were included in our study. Samples were taken before chemotherapy, both at diagnosis and at the time of the first relapse, with written informed consent. Leukemic blast cells were separated from bone marrow and/or peripheral blood samples by Ficoll–Conray density gradient centrifugation (density 1.077 g/ml) and then the RNA was isolated.

2.8. Statistical analysis

Differences in cell cycles and cell numbers between the siRNA-treated group and the control group in K562 cells were evaluated by two-sample *t* tests. The expression of PRAME and the percentages of cells in S phase were compared between the diagnosis and relapse samples using the two-sided Wilcoxon rank sum test. The results presented are the mean ± SD of three independent experiments. A statistically significant result was considered to have a *P*-value of <0.05.

Table 1
Cell cycle analysis of PRAME siRNA transfected in K562 cells.

	G_0/G_1 (%)	S (%)	G_2/M (%)
Day 1			
Control	25.7 ± 1.8	56.2 ± 1.8	18.1 ± 1.1
PRAME siRNA	36.6 ± 0.2***	50.4 ± 0.4**	13.2 ± 0.6**
Day 2			
Control	37.4 ± 1.2	52.6 ± 0.1	10.0 ± 1.2
PRAME siRNA	50.7 ± 1.3***	41.8 ± 1.6***	7.5 ± 0.3*
Day 3			
Control	44.7 ± 2.0	49.3 ± 1.1	6.0 ± 1.2
PRAME siRNA	59.2 ± 2.5***	35.3 ± 2.7***	5.5 ± 1.7

Cellular DNA content was evaluated after PI staining of during day 1 to day 3 of culture.
Mean ± SD of three experiments.
* $P < 0.05$ vs. control.
** $P < 0.005$ vs. control.
*** $P < 0.001$ vs. control.

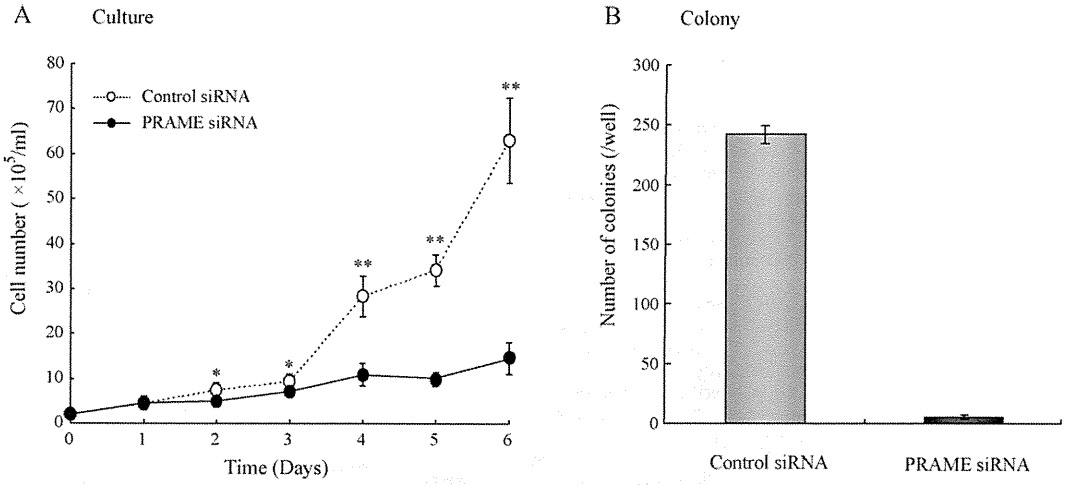

Fig. 2. Cell proliferation of PRAME siRNA-treated K562 cells. (A) The number of PRAME siRNAtreated cells (-●-) and control siRNA cells (-○-) in liquid culture from day 1 to day 6 (**$P < 0.005$, *$P < 0.05$). (B) The number of colonies of PRAME siRNA-treated cells (black bar) and control siRNA cells (gray bar) which were counted at day 7 after plating. The number of colonies significantly decreased in PRAME siRNA-treated cells. The graph shows the results from one of three independent experiments.

3. Results

3.1. Inhibition of PRAME expression

After 1 day of transfection, the efficiency of PRAME siRNA silencing was analyzed by flow cytometry using a control pmaxGFP plasmid marker. The efficiency of transfection in siRNA-treated K562 cells was more than 90%. Cell viabilities examined at day 1 were not significantly different between PRAME siRNA-treated cells, control siRNA-treated cells, and untreated cells. PRAME siRNA knockdown resulted in a reduction of *PRAME* mRNA expression of >70% from day 1 to day 3 (Fig. 1A). The western blot analysis demonstrated almost complete inhibition of PRAME protein expression, and this inhibition was maintained from day 1 to day 6 after PRAME siRNA transfection (Fig. 1B). The *PRAME* mRNA and protein levels did not change in the untreated cells or in the control siRNA-treated cells.

3.2. Cell growth and morphology

As shown in Fig. 2A, significant inhibition of cell proliferation was observed in transfected cells with PRAME siRNA, especially from day 4 to day 6. RNA interference-induced knockdown of *PRAME* expression also resulted in a significant decrease of clonogenic growth of K562 cells (Fig. 2B). The colony size was also smaller in PRAME siRNA-treated cells compared to that of control cells (data not shown). Morphological changes were recognized after day 3, with the reduction of cytoplasmic basophilia and changes to the nuclear shape observed. Also, apoptotic-like cells among PRAME siRNA-treated cells were observed between day

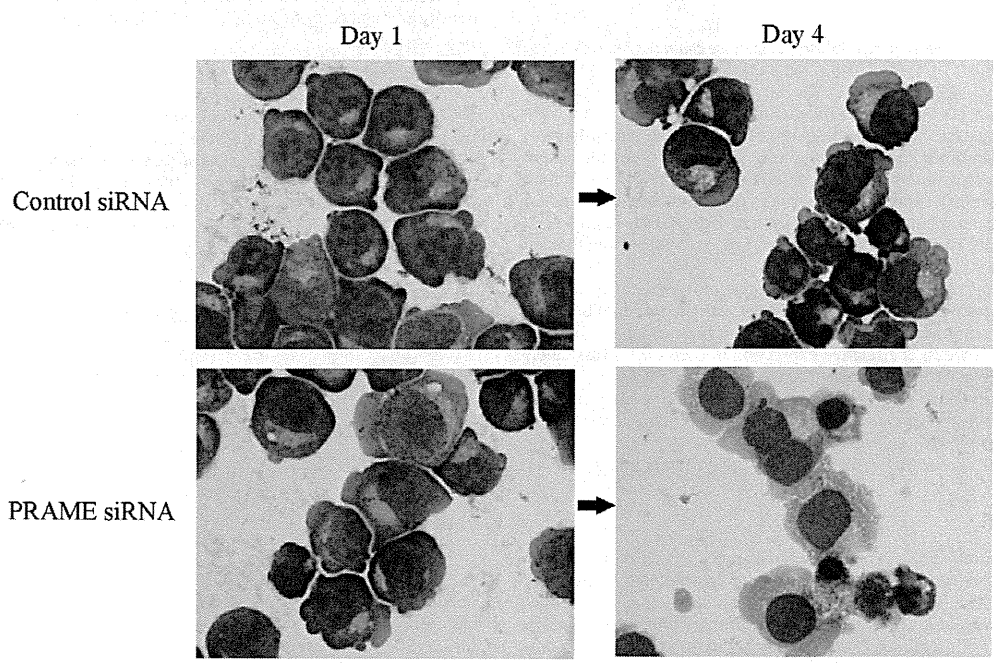

Fig. 3. Morphology of PRAME siRNA-treated K562 cells. Morphological examination in PRAME siRNA-treated cells revealed the appearance of apoptotic cells, a reduction of cytoplasmic basophilia and nuclear shape changes at day 4. The cytospin preparations were stained with May–Grünwald–Giemsa.

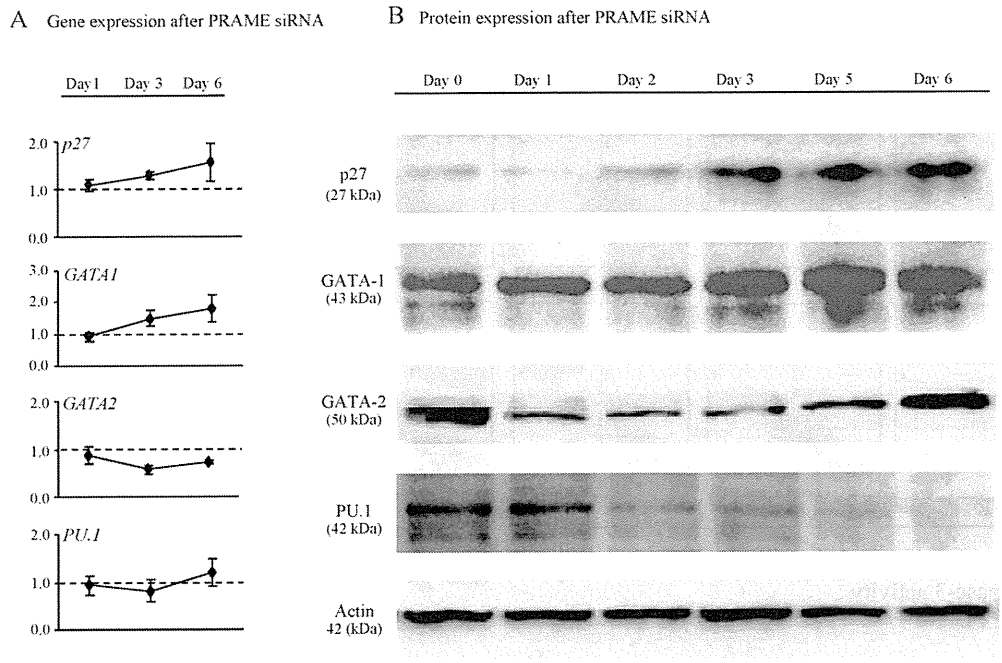

Fig. 4. Changes in gene expression and western blot analysis after PRAME siRNA transfected K562 cells. (A) Changes in *p27*, *GATA1*, *GATA2* and *PU.1* gene expression as the average ratio of PRAME siRNA-treated cells relative to the corresponding control cells on day 1, day 3 and day 6 from a TaqMan gene assay. (B) Expression of protein shown from day 0 to day 6 after PRAME siRNA transfection. The protein expression of p27 increased by day 3 through day 6. GATA-1 increased by day 3 through day 6, GATA-2 decreased by day 1 through day 5, and PU.1 protein expression decreased by day 2 through day 6.

4 and day 6, but were not observed among the control cells (Fig. 3).

3.3. Cell cycle analysis, cell cycle-related gene and protein level

Cell cycle analysis showed that PRAME knockdown in K562 led to a significant increase of cells in G_0/G_1 phase associated with a decreased number of cells in S phase, in comparison with control cells, from day 1 to day 3, as shown in Table 1. Among the cell cycle related genes analyzed with a TaqMan gene assay, a clear increase of *p27* expression was observed between day 3 and day 6 (Fig. 4A). By western blot analysis, an increase of p27 protein expression from day 3 to day 6 was also confirmed with the inhibition of PRAME protein expression (Fig. 4B).

3.4. Apoptosis-related gene expression and protein level

To evaluate whether the decrease in cell viability after siRNA treatment resulted from apoptosis, the percentage of annexin V-positive fractions were determined from day 1 to day 6 after treatment with PRAME siRNA or control siRNA in K562 cells. The percentage of apoptotic cells gradually increased from day 3 to day 6 in PRAME siRNA-treated cells (Fig. 5A). We found that the total percentage of apoptotic cells on day 6 was $50.8 \pm 6.1\%$ (early apoptotic cells $38.8 \pm 5.7\%$, late apoptotic/necrotic cells $12.0 \pm 1.3\%$) in PRAME siRNA-treated cells and only $15.3 \pm 4.5\%$ (early apoptosis $12.8 \pm 4.2\%$, late apoptosis $2.5 \pm 0.5\%$) in control cells.

Since it is known that caspase-3 plays a crucial role in apoptosis, the enzymatic activity of caspase-3 after PRAME siRNA was measured by using an antibody against cleaved caspase-3 with flow cytometry. Fig. 5B shows that caspase-3 was activated on day 3 in PRAME siRNA-treated cells, then increased gradually with the maximum activity being observed on day 6 (33.4%). Western blot analysis showed that a faint band of cleaved caspase-3 protein was detected on day 3, then an obviously augmented band was observed on days 5 and 6 (Fig. 5C). Furthermore, we examined the apoptosis of PRAME siRNA-treated cells by using z-VAD-fmk (a general pan-specific caspase inhibitor) or z-DEVD-fmk (a specific inhibitor of the caspase-3-like enzyme). As a result, apoptosis was partially blocked but not completely. The total mean percentage of annexin V positive cells on day 6 was 36.2% (early apoptosis 32.8%, late apoptosis 3.4%) with z-VAD-fmk, and 38.3% (early apoptosis 32.5%, late apoptosis 5.8%) with z-DEVD-fmk, despite successful blocking of caspase-3 activity in both (data not shown).

3.5. Differentiation-related gene expression and protein level

To address whether siRNA PRAME transfection induces differentiation of leukemic cells, the expression of several genes related to myeloid and erythroid differentiation was analyzed. From TaqMan gene assay results, we observed an increase of *GATA-1* expression and a decrease of *GATA-2* expression in PRAME siRNA-treated cells at day 3 (Fig. 4A). A change in *PU.1* mRNA expression was not clear because its expression levels were very low in the K562 cells. Western blotting confirmed an increase in GATA-1 protein from day 3 to day 6, a decrease in GATA-2 protein from day 1 to day 5, and a decrease in PU.1 protein from day 2 to day 6 (Fig. 4B). No significant differences were observed in the differentiation-related gene expression or protein level between PRAME siRNA cells and PRAME siRNA cells plus z-VAD-fmk (Supplementary Fig. 1).

3.6. PRAME expression and cell cycle profiles in clinical samples

PRAME mRNA expression in paired leukemia samples was also analyzed using quantitative real-time RT-PCR. The *PRAME* expression was not statistically different at relapse compared to at diagnosis (Fig. 6A).

As PRAME siRNA transfection led to a significant decrease of K562 cells in S phase, we examined the relationship between

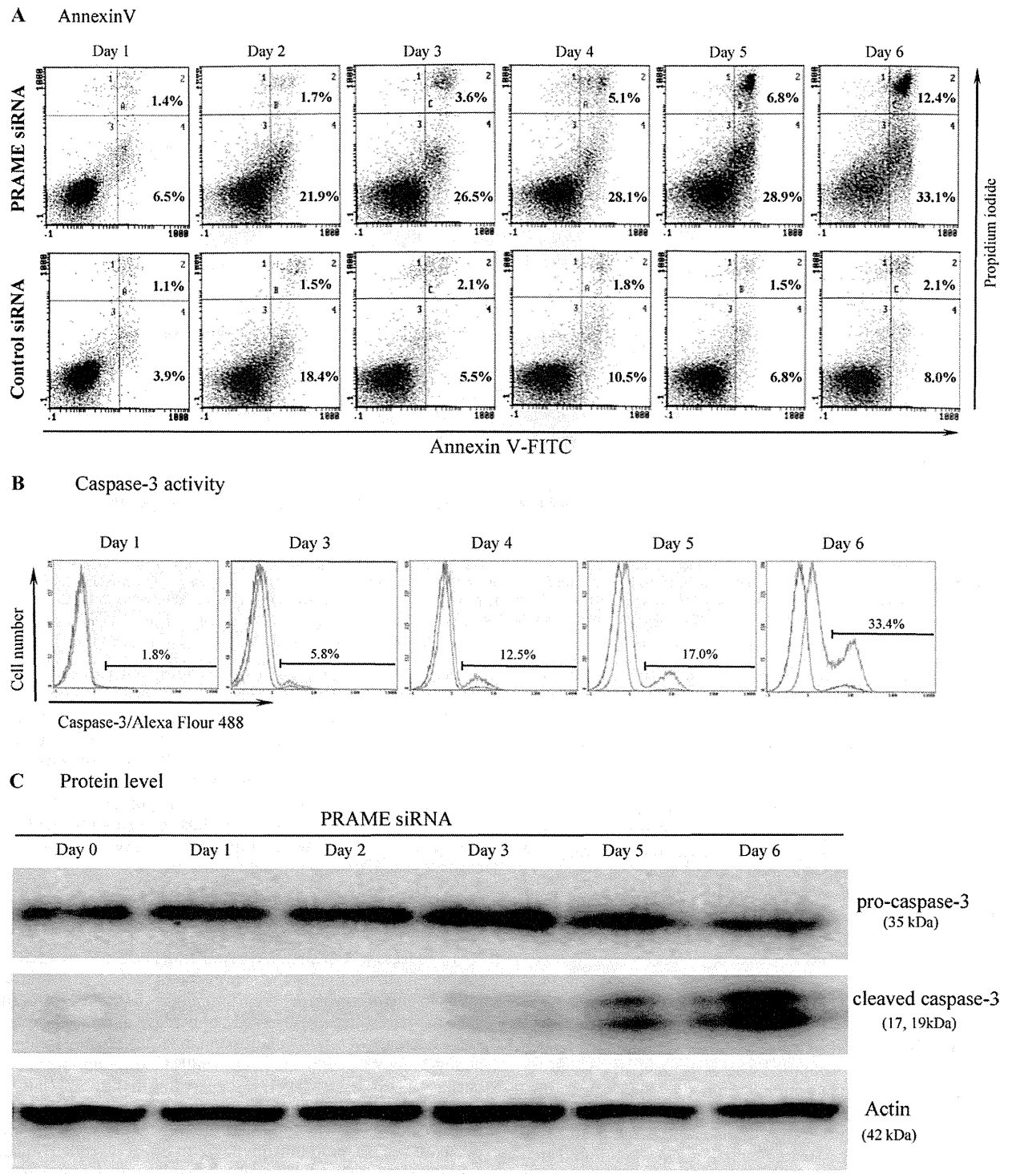

Fig. 5. Determination of apoptotic cells after PRAME siRNA transfection in K562 cells. (A) Annexin V-FITC/PI staining from day 1 to day 6 of the culture in PRAME siRNA (upper lane) and the control siRNA cells (lower lane). The lower right quadrant represents the early apoptotic cells and the upper right quadrant contains the late apoptotic cells. The annexin V/FITC positive fraction of PRAME siRNA-treated cells gradually increased by day 3 through day 6, in comparison with that of the control cells. The results show one of three independent experiments. (B) Caspase-3 activity measured by flow cytometry. Data indicated that caspase-3 activity was activated at day 3, and then increased gradually from day 4 to day 6 in comparison with control cells. (C) The protein expression of cleaved caspase-3 detected by western blotting. A slight increase of cleaved caspase-3 protein expression was observed from day 3, and obvious augmentation was detected at day 5 and day 6.

PRAME expression and the percentage of leukemic cells in S phase for paired samples. The percentage of leukemic cells in S phase was not statistically different at relapse compared to at diagnosis. For further analysis, the cases were divided into two groups at the median (1.22 fold) of the increase in the ratio of *PRAME* mRNA expression. In the group with the greater increases ($\geq$1.22) of *PRAME* mRNA expression at relapse, as shown in Fig. 6B, the percentages of S phase cells at relapse had significantly increased

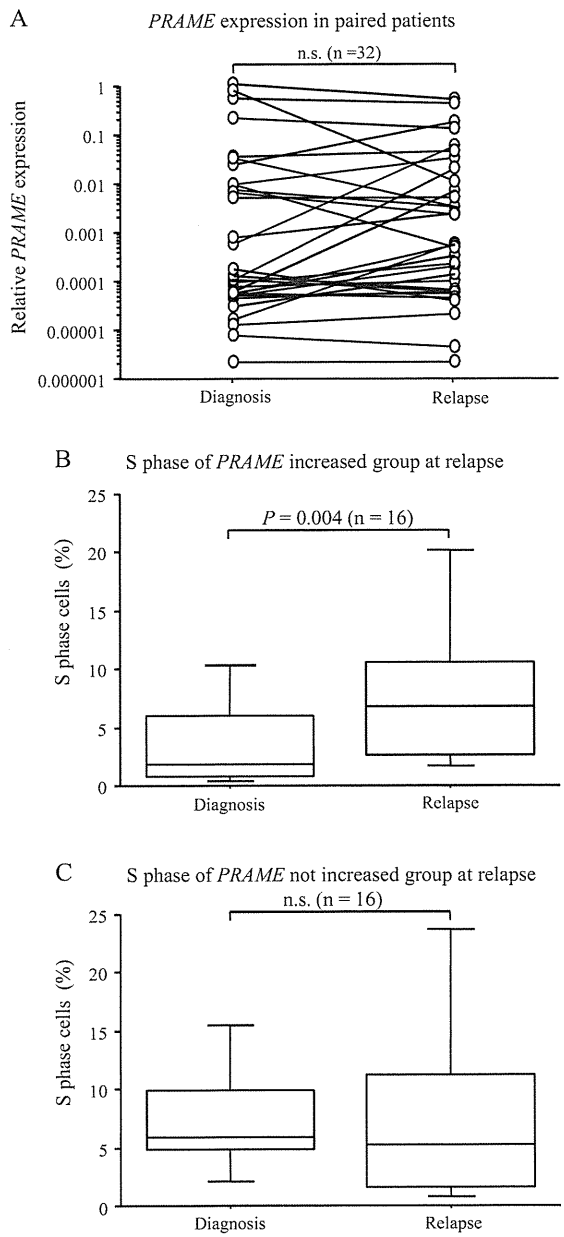

Fig. 6. *PRAME* mRNA expression and leukemic blast cells at S phase of the cell cycle for paired acute leukemia patient samples. Thirty-two cases were dichotomized at the median of the relapse/diagnosis ratio of *PRAME* mRNA expression. (A) *PRAME* mRNA expression at relapse was not statistically different compared to that at diagnosis. (B) The subgroup in which the relapse/diagnosis ratio of *PRAME* mRNA expression was ≥1.22 fold. The percentages of S phase cells at relapse increased significantly compared to that at diagnosis. The median values of S phase cells were 1.9% (at diagnosis) and 6.8% (at relapse) ($P = 0.004$, $n = 16$). (C) The subgroup in which relapse/diagnosis ratio of *PRAME* mRNA expression was <1.22 fold. The percentages of S phase cells were not statistically different at relapse compared to that at diagnosis (5.8% at diagnosis vs. 5.2% at relapse, $P = 0.66$, $n = 16$). The large boxes represent the interquartile range (25th–75th percentile), and the lines inside the boxes denote the median. The upper and lower bars represent the 10th–90th percentile of the samples studied.

compared to at diagnosis ($P = 0.004$, $n = 16$). In the other group in which *PRAME* expression did not increase (<1.22) at relapse compared to at diagnosis, the percentages of S phase cells were not statistically different at relapse compared to at diagnosis (Fig. 6C).

4. Discussion

We examined whether PRAME expression had an effect on cell proliferation and differentiation in K562 cells by transfection with siRNA. In this study, we observed that there was a significant decrease in the colony formation of the PRAME siRNA-treated cells, as well as a decrease in the growth rate in liquid culture. In the cell cycle analysis, a significant decrease of cells in S phase and an increase of cells in G_0/G_1 phase were simultaneously observed in PRAME siRNA-treated cells, suggesting PRAME knockdown was associated with cell cycle arrest in the G_0/G_1 phase. The cell cycle arrest observed was likely caused by the increased p27 mRNA and protein expression levels, as it is well known that p27 plays an essential role to arrest the cell cycle [18]. Our results are in agreement with a previous report that found the percentage of cells in G_0/G_1 phase was significantly decreased in PRAME transfected KG-1 cells, which is a PRAME negative cell line [13]. The cell cycle arrest was followed by an increase of annexin V positive cells. In addition, the increases in caspase-3 activity and cleaved caspase-3 protein were consistent with the increase of apoptotic cells in the same period after transfection. However, the result of PRAME siRNA with caspase-3 inhibitor suggests that the apoptosis is not only caspase-3 dependent but also has other pathways.

Our present results show increased GATA-1 protein levels and decreased GATA-2 and PU.1 protein levels in PRAME siRNA-treated K562 cells. The PU.1 has an antagonistic function in the development of distinct hematopoietic lineages with GATA factors. GATA-1 blocks PU.1 transactivation and ensures the continued maturation of erythroid and megakaryocytic cells [19,20]. GATA-2 is detected at an early stage in hematopoietic development and decreases according to the progression of erythroid differentiation [21]. Erythroid differentiation is reported to accompany the increase of GATA-1 and the decrease of GATA-2 and PU.1, as we could show in our study by silencing PRAME expression.

There are reports which show that PRAME silencing promotes cell proliferation in K562. Oehler et al. reported that PRAME silencing suppressed the cell growth of HL60 cells but promoted cell proliferation in K562 [12]. However, in their report, PRAME silenced K562RARA cells (K562 cells with increased numbers of RARα receptors) showed no apparent difference in proliferation compared with the control cells in their study with no ATRA exposure (reported in supplemental data). Moreover, our data showed that the PRAME silencing suppressed the K562 cell growth especially in colony assays, in which the incubation period is longer than theirs. Tajeddine et al. reported on the proliferative effect of PRAME siRNA in vivo, from a tumor transplantation study on mice [13]. It is possible that PRAME silencing may act differently in vivo than in vitro. For example, it is known that an immunological reaction against PRAME may occur in vivo [22,23].

Since these effects originated with the appearance of the cell cycle arrest, we analyzed the correlation between the *PRAME* expression level and the population of S phase cells in paired acute leukemia samples. In this study, the *PRAME* expression level increased at relapse compared with at diagnosis in approximately half of the paired samples. In the group in which the *PRAME* expression increased at relapse, the percentages of S phase cells at relapse significantly increased compared to at diagnosis. These findings agree with the results of our present cell line studies. Thus, increased expression of *PRAME* in leukemic cells at relapse may lead to cell cycle progression and cell proliferation. It was reported that the progression of chronic phase CML to advanced phase CML was accompanied by new gene expressions occurring before the accumulation of leukemic blast cells [9]. This report showed a significant association between PRAME and the progression of CML. Similarly, another report showed that genetic aberrations in advanced stage CML correlate with PRAME expression, and PRAME expression was

associated with a significantly reduced overall survival [24]. Considering that PRAME expression increases at blastic crisis, certain populations of acute leukemia cases may also acquire more aggressive characteristics at relapse with an increase of PRAME. Thus, PRAME may have a role in disease progression in acute leukemia.

In conclusion, inhibition of PRAME by siRNA in K562 cells, from our data, suggests that PRAME expression is associated with cell cycle progression from the G_0/G_1 phase to the S phase, as well as with the inhibition of apoptosis and the blocking of erythroid differentiation. Furthermore, we found cell cycle progression in acute leukemia patients in whom *PRAME* expression became higher at relapse than at diagnosis. The *PRAME* gene may be important for the proliferation of leukemic cells. Although the details of the functional mechanisms of PRAME in vivo needs further investigation, insights into the function of PRAME can be expected to provide a new perspective on the characteristics of relapse, making it an attractive molecular target for potential therapy.

Conflict of interest statement

The authors indicated no conflicts of interest.

Acknowledgement

This study was supported in part by a grant-in-aid from the Tokyo Women's Medical University Institute for Integrated Medical Sciences (TIIMS).

Contributions: N.T. performed experiments, analyzed and interpreted the data, and wrote the manuscript. Y.W. designed the research, performed experiments, interpreted results and helped with writing the manuscript. M.S. and M.T. helped with collecting samples and analyzing the data. T.M. helped with the design of research and modified the initial drafts of the manuscript.

Appendix A. Supplementary data

Supplementary data associated with this article can be found, in the online version, at doi:10.1016/j.leukres.2011.04.005.

References

[1] Ikeda H, Lethe B, Lehmann F, van Baren N, Baurain JF, de Smet C, et al. Characterization of an antigen that is recognized on a melanoma showing partial HLA loss by CTL expressing an NK inhibitory receptor. Immunity 1997;6:199–208.
[2] van Baren N, Chambost H, Ferrant A, Michaux L, Ikeda H, Millard I, et al. PRAME, a gene encoding an antigen recognized on a human melanoma by cytolytic T cells, is expressed in acute leukaemia cells. Br J Haematol 1998;102:1376–9.
[3] van't Veer LJ, Dai H, van de Vijver MJ, He YD, Hart AA, Mao M, et al. Gene expression profiling predicts clinical outcome of breast cancer. Nature 2002;415:530–6.
[4] Oberthuer A, Hero B, Spitz R, Berthold F, Fischer M. The tumor-associated antigen PRAME is universally expressed in high-stage neuroblastoma and associated with poor outcome. Clin Cancer Res 2004;10:4307–13.
[5] Epping MT, Hart AA, Glas AM, Krijgsman O, Bernards R. PRAME expression and clinical outcome of breast cancer. Br J Cancer 2008;99:398–403.
[6] Greiner J, Ringhoffer M, Taniguchi M, Li L, Schmitt A, Shiku H, et al. mRNA expression of leukemia-associated antigens in patients with acute myeloid leukemia for the development of specific immunotherapies. Int J Cancer 2004;108:704–11.
[7] Paydas S, Tanriverdi K, Yavuz S, Disel U, Baslamisli F, Burgut R. PRAME mRNA levels in cases with acute leukemia: clinical importance and future prospects. Am J Hematol 2005;79:257–61.
[8] Watari K, Tojo A, Nagamura-Inoue T, Nagamura F, Takeshita A, Fukushima T, et al. Identification of a melanoma antigen PRAME, as a BCR/ABL inducible gene. FEBS Lett 2000;466:367–71.
[9] Radich JP, Dai H, Mao M, Oehler V, Schelter J, Druker B, et al. Gene expression changes associated with progression and response in chronic myeloid leukemia. Proc Natl Acad Sci USA 2006;103:2794–9.
[10] Steinbach D, Schramm A, Eggert A, Onda M, Dawczynski K, Rump A, et al. Identification of a set of seven genes for the monitoring of minimal residual disease in pediatric acute myeloid leukemia. Clin Cancer Res 2006;12:2434–41.
[11] Epping MT, Wang L, Edel MJ, Carlee L, Hernandez M, Bernards R. The human tumor antigen PRAME is a dominant repressor of retinoic acid receptor signaling. Cell 2005;122:835–47.
[12] Oehler VG, Guthrie KA, Cummings CL, Sabo K, Wood BL, Gooley T, et al. The preferentially expressed antigen in melanoma (PRAME) inhibits myeloid differentiation in normal hematopoietic and leukemic progenitor cells. Blood 2009;114:3299–308.
[13] Tajeddine N, Gala JL, Louis M, Van Schoor M, Tombal B, Gailly P. Tumor-associated antigen preferentially expressed antigen of melanoma (PRAME) induces caspase-independent cell death in vitro and reduces tumorigenicity in vivo. Cancer Res 2005;65:7348–55.
[14] Robertson KA, Mueller L, Collins SJ. Retinoic acid receptors in myeloid leukemia: characterization of receptors in retinoic acid-resistant K-562 cells. Blood 1991;77:340–7.
[15] Motoji T, Takanashi M, Motomura S, Wang YH, Shiozaki H, Aoyama M, et al. Growth stimulatory effect of thrombopoietin on the blast cells of acute myelogenous leukemia. Br J Haematol 1996;94:513–6.
[16] Wang YH, Takanashi M, Tsuji K, Tanaka N, Shiseki M, Mori N, et al. Level of DNA topoisomerase IIα mRNA predicts the treatment response of relapsed acute leukemic patients. Leuk Res 2009;33:902–7.
[17] Kotaki M, Motoji T, Takanashi M, Wang YH, Mizoguchi H. Anti-proliferative effect of the abl tyrosine kinase inhibitor STI571 on the P-glycoprotein positive K562/ADM cell line. Cancer Lett 2003;199:61–8.
[18] Polyak K, Kato JY, Solomon MJ, Sherr CJ, Massague J, Roberts JM, et al. p27Kip1, a cyclin-Cdk inhibitor, links transforming growth factor-beta and contact inhibition to cell cycle arrest. Genes Dev 1994;8:9–22.
[19] Kitajima K, Tanaka M, Zheng J, Yen H, Sato A, Sugiyama D, et al. Redirecting differentiation of hematopoietic progenitors by a transcription factor, GATA-2. Blood 2006;107:1857–63.
[20] Friedman AD. Transcriptional control of granulocyte and monocyte development. Oncogene 2007;26:6816–28.
[21] Testa U. Apoptotic mechanisms in the control of erythropoiesis. Leukemia 2004;18:1176–99.
[22] Greiner J, Schmitt M, Li L, Giannopoulos K, Bosch K, Schmitt A, et al. Expression of tumor-associated antigens in acute myeloid leukemia: implications for specific immunotherapeutic approaches. Blood 2006;108:4109–17.
[23] Quintarelli C, Dotti G, De Angelis B, Hoyos V, Mims M, Luciano L, et al. Cytotoxic T lymphocytes directed to the Preferentially Expressed Antigen of Melanoma (PRAME) target chronic myeloid leukemia. Blood 2008;112:1876–85.
[24] Luetkens T, Schafhausen P, Uhlich F, Stasche T, Akbulak R, Bartels BM, et al. Expression, epigenetic regulation, and humoral immunogenicity of cancer-testis antigens in chronic myeloid leukemia. Leuk Res 2010;34:1647–55.

Original Paper

Acta Hæmatologica

Acta Haematol 2011;126:69–75
DOI: 10.1159/000324932

Received: October 13, 2010
Accepted after revision: February 7, 2011
Published online: April 13, 2011

Absence of Mutations on the *SNF5* Gene in Hematological Neoplasms with Chromosome 22 Abnormalities

Naoki Mori[a] Kaoru Inoue[a] Michiko Okada[b] Toshiko Motoji[a]

[a]Department of Hematology, Tokyo Women's Medical University, [b]Chromosome Laboratory, Shiseikai Dai-ni Hospital, Tokyo, Japan

Key Words

Hematological neoplasms · Allelic loss · SNF5 · Chromosome 22 · Tumor suppressor gene · Chromatin remodeling

Abstract

Background: The relation with *SNF5* mutation and chromosome 22 abnormalities is not clear in hematological neoplasms. ***Methods:*** To elucidate the relevance of the *SNF5* gene on 22q11.2, karyotypes were reviewed in 283 hematological neoplasms. Loss of heterozygosity (LOH) on 22q was analyzed in 21 plasma cell myelomas without chromosome 22 abnormalities. Polymerase chain reaction-single strand conformation polymorphism (PCR-SSCP) on the *SNF5* gene was analyzed in 8 hematological neoplasms with 22q- or -22, and 8 chronic myelogenous leukemias (CMLs) in blast crisis. Fluorescence in situ hybridization (FISH) was performed in 1 myelodysplastic syndrome (MDS) case with -22,del(22)(q11.2 q13). ***Results:*** 22q- or -22 was observed in 36 patients. LOH on 22q was detected in 1 of the 21 myelomas. Mobility shifts were found by PCR-SSCP analysis in 2 CMLs, whereas sequence analysis showed polymorphisms. FISH analysis revealed the *SNF5* gene was not deleted in the MDS case. ***Conclusion:*** These results suggest that alterations of the *SNF5* gene are rare in hematological neoplasms with chromosome 22 abnormalities. Haploinsufficiency may contribute to the development of these neoplasms.

Introduction

Mounting evidence has shown that inactivation of tumor suppressor genes is closely associated with tumorigenesis in a wide variety of human tumors [1]. The two-mutation hypothesis suggests that both alleles of a tumor suppressor gene are inactivated in tumors [2]. Inactivation of a tumor suppressor gene is often caused by a mutation, a small deletion of one allele accompanied by loss of another allele. Loss of heterozygosity (LOH) has been reported to occur in various chromosomal regions in diverse tumor types. We previously reported the allelotype in the progression of chronic myelogenous leukemia (CML), *BCR-ABL1*-positive and myelodysplastic syndrome (MDS) [3, 4]. Frequent LOH was found on the short arm of chromosome 1 (1p); however, LOH on the long arm of chromosome 22 (22q) was also observed in a proportion of the disorders [3, 4].

The *SNF5* gene encodes a member of the SW1/SNF chromatin remodeling complex [5–7]. The *SNF5* gene is located on 22q11.2. Truncating mutations on one allele of the gene were frequently detected in aggressive rhabdoid tumors (RT) and another allele was eventually lost [8]. Mutations were also found in choroid plexus carcinomas and medulloblastomas, but not in breast cancers, Wilms' tumors or gliomas [9]. Furthermore, homozygous knockout of snf5 results in embryonic lethality, whereas heterozygous mice develop tumors consistent with RT [10].

KARGER

Fax +41 61 306 12 34
E-Mail karger@karger.ch
www.karger.com

0001–5792/11/1262–0069$38.00/0

Accessible online at:
www.karger.com/aha

Naoki Mori, MD, PhD
Department of Hematology
Tokyo Women's Medical University
8-1 Kawada-cho, Shinjuku-ku, Tokyo 162-8666 (Japan)
Tel. +81 3 3353 8111, E-Mail mori@dh.twmu.ac.jp

Table 1. Clinical characteristics of hematological neoplasms with 22q- or -22, and CML blast crisis

No.	Age/sex	Disease	Karyotype
1	49/M	AML[1]	43,XY,-1,-11,-17,-17,-21,-22, +mar1,+mar2,+mar3
2	62/M	AML[1]	43,t(X;5)(q26;q15),Y,der(1)t(1;12)(q44;p11.2),-5,-7, der(11)t(1;11)(p11;q21),der(12)t(12;?)(p11.2;?), der(12)t(12;?)(q24.3;?),-15,der(19)t(19;?)(p10;?), der(21)t(21;?)(q22;?),-22,+der(?)t(22;?)(q11.2;?)/46,XY
3	58/M	plasma cell myeloma	35~36,X,add(Y)(q12)[7]-1[7], der(1)add(1)(p36)add(1)(q11)[7]-6[7], del(7)(q32q34)[6]-8[7], add(8)(q24.3)[5],-10[6], add(10)(q26)[6], del(11)(q23)[4],-12[7],-13[7], add13(p11)[7],-14[6],-16[7],-17[7],-17[7],-17[7],-20[7], del(20)(q13)[6],-22[5], del(22)(q11.2)[2],+2~6mar[5]cp7)[31]/46,XY[7]
4	76/F	lymphoplasmacytic lymphoma	46,XX,t(11;18)(q21;q21.1)[21]/47,idem,+del(22)(q11.2)[3]/46,XX[2]
5	60/F	plasma cell myeloma	38~39,X,-X,add(1p),del(1p),-2,-3,-5,-5,-8,+10, add(14q),16,-16,-17,-19, -22,-22,+mar1,+mar2,+mar3,+mar4,+1-2mar[33]/46,XX[18]
6	78/M	RAEB-2	44,XY,del(5)(q1?2;q22),der(7)add(7)(p22)del(7)(q11.2),der(12)t(12;13)(p13;q11),-13,der(14)t(1;14)(q21;p12),-15,-18,-22,+2mar[27]/46,XY[2]
7	39/F	plasma cell myeloma	42~44XX, t(1;13)(p22;q14),-11,der(11)del(11)(p11p13)del(11)(q2?2.2q23~25)[4], add(14)(q32)[2],-17[3],-17[2], del(18)(q21q23)[2],-19[3],-22[4],+mar1[4],+1~3mar[4](cp4)
8	77/F	B lymphoblastic leukemia/lymphoma NOS	45XX,-9,-22,+del(9q+)(p13?)
9	62/F	CML BC	46,XX,t(9;22)(q34;q11.2)
10	50/F	CML BC	46,XX,t(9;22)(q34;q11.2)
11	38/M	CML BC	46,XY,t(9;22)(q34;q11.2)
12	46/M	CML BC	46,XY,t(9;22)(q34;q11.2)
13	34/M	CML BC	46,XY,t(9;22)(q34;q11.2)
14	41/M	CML BC	46,XY,t(3;21)(q27;q22),t(10;9;22)(q22;q34;q11.2)
15	58/M	CML BC	46,XY,t(9;22)(q34;q11.2)[14]/47,idem,+der(22)t(9;22)(q34;q11.2)[17]
16	72/M	CML BC	46,XY,t(9;22)(q34;q11.2)

[1] AML with myelodysplasia-related changes.

More recently, a conditional knockout mouse model showed high incidence of CD8+ lymphoma [11]. In hematological neoplasms, previous fluorescence in situ hybridization (FISH) analysis indicated that the gene was deleted in CML [12]. Deletions of chromosome arms 9q and/or 22q have been detected in CML and these deletions were associated with poor prognosis [13]. In addition, *SNF5* mutation was detected in a case of malignant lymphoma and some leukemia cell lines [14]; however, *SNF5* mutation was absent in acute myeloid leukemia (AML) [15]. So far the relation with *SNF5* mutation and chromosome 22 abnormalities is not clear in hematological neoplasms. To elucidate the relevance of SNF5 in hematological neoplasms with chromosome 22 abnormalities, we analyzed karyotypes and performed polymerase chain reaction-single strand conformation polymorphism (PCR-SSCP) analysis on the *SNF5* gene in CML blast crisis (BC) and other hematological neoplasms with -22 or 22q-.

Patients and Methods

Cytogenetic Analysis

Karyotypes were reviewed in 283 patients with hematological neoplasms. The 283 neoplasms consisted of 124 CMLs, *BCR-ABL1*-positive (15 BC); 2 AMLs with t(8;21)(q22;q22), *RUNX1-*

Table 2. Primers of the *SNF5* gene

Primer	Sequence	Size of PCR products, bp
Exon 1	5′-ATTTCGCCTTCCGGCTTCG-3′ 5′-ATGAATGGAGACGCGCGCT-3′	292
Exon 2	5′-GTGCTGCGACCCTTATAATG-3′ 5′-CATGACATAAGCGAGTGGTT-3′	235
Exon 3	5′-CTTGATGTGCTGCATCCACT-3′ 5′-ACAGGTGTCCCCAGAGATG-3′	252
Exon 4	5′-AGGATCAGGTCCTATACTGA-3′ 5′-GAACTAAGGCGGAATCAGCA-3′	237
Exon 5	5′-ATTTGCATACCTAGGGCTCC-3′ 5′-GGACTGTTCCCACGTAACA-3′	250
Exon 6	5′-CCAAGCATGGTGCAATCTCT-3′ 5′-TCAGTGCTCCATGATGACAC-3′	284
Exon 7	5′-AAGCTCTAACTTGTGTCCTTT-3′ 5′-AGGGAGAGACTCATGCATGAT-3′	252
Exon 8	5′-GAGGATTCTCCATCTATAGC-3′ 5′-TGGAAAGCCAGGTGCCTGT-3′	243
Exon 9	5′-TGTTCCCACCCCTACACTTG-3′ 5′-GCAGGACTGGGGCTCAAC-3′	327

RUNX1T1; 25 AMLs with myelodysplasia-related changes; 5 AMLs, not otherwise specified (NOS); 5 refractory anemias; 6 refractory cytopenias with multilineage dysplasia; 5 refractory anemias with excess blasts (RAEB)-1; 7 RAEB-2; 5 MDS, unclassifiable; 10 B lymphoblastic leukemia/lymphomas with t(9;22)(q34;q11.2), *BCR-ABL1*; 7 B lymphoblastic leukemia/lymphomas, NOS; 6 T lymphoblastic leukemia/lymphomas; 32 plasma cell myelomas; 16 diffuse large B-cell lymphomas; 9 follicular lymphomas; 2 lymphoplasmacytic lymphomas; 2 Burkitt lymphomas; 6 adult T-cell leukemia/lymphomas; 5 peripheral T-cell lymphomas, NOS; 2 angioimmunoblastic T-cell lymphomas; and 2 anaplastic large cell lymphomas according to the World Health Organization 2008 classification. Cytogenetic analysis was performed according to standard methods. Chromosome preparations were Q-banded and karyotypes were described according to the International System for Human Cytogenetic Nomenclature (ISCN 2009). Thirty metaphases were evaluated in most samples.

Extraction of DNA

Bone marrow or peripheral blood samples were obtained from 16 of the 283 patients with hematological neoplasms for PCR-SSCP analysis. The 16 neoplasms consisted of 8 hematological malignancies with 22q- or -22 (2 AMLs with myelodysplasia-related changes, 3 plasma cell myelomas, 1 lymphoplasmacytic lymphoma, 1 RAEB-2 and 1 B lymphoblastic leukemia/lymphoma, NOS) and 8 patients with CML BC (table 1). Paired samples of myeloma cells and lymphocytes from the same individual were available for LOH analysis in 21 of the 32 patients with plasma cell myeloma. Mononuclear cells were isolated from bone marrow or peripheral blood by Ficoll-Conray gradient centrifugation. Genomic DNA was prepared by proteinase K digestion and phenol/chloroform extraction or using a QIAamp DNA Blood Mini Kit (Qiagen, Valencia, Calif., USA).

LOH Analysis

PCR-amplification of microsatellite sequences was used to determine LOH. Primers for these microsatellite sequences were obtained from Research Genetics (Huntsville, Ala., USA) [16]. Loci analyzed were as follows: 22q, *D22S420, D22S446, D22S280, D22S274* and *D22S1169*. Each PCR reaction contained 10 ng of DNA, 5 pmol of each primer, 2 nmol of each of dNTPs, 0.3 units of Taq DNA polymerase (Takara, Ohtsu, Japan) and 2 μCi of [α-^{32}P]dCTP (Amersham, Japan) in 10 μl of the specified buffer with 1.5 mM $MgCl_2$. Thirty-two cycles of amplification, polyacrylamide gel electrophoresis and autoradiography were performed as previously published [3, 4]. LOH was scored in informative cases if a significant reduction (>50%) in the signal of the allele from the myeloma sample was noted in comparison with the corresponding allele in the adjacent lane from lymphocytes of the same individual. In samples showing LOH, PCR amplification and analysis were repeated to insure consistency of results. We performed duplex PCR to compare the intensity of 2 loci.

PCR-SSCP Analysis

For PCR-SSCP analysis, PCR was performed with 3 μCi of [α-^{32}P]dCTP (Amersham) to the PCR mixture [17]. Labeled PCR mixture was heated at 94°C for 5 min, chilled on ice and loaded on a 6% neutral polyacrylamide gel containing 90 mM Tris-borate and 2 mM EDTA either with or without 10% glycerol. After electrophoresis at 400 V for 16 h, the gel was dried and exposed to X-ray film at –80°C for 1–3 days, with an intensifying screen. Sequences of primers for the *SNF5* gene are listed in table 2.

Sequencing

Sequencing was performed in both directions on the MegaBase sequence system (Amersham, Buckingham, UK). PCR products were purified using a QIAQuick PCR Purification Kit (Qiagen) and ligated into pGEM-T vector (Promega, Madison, Wisc., USA). As a template, one of the plasmid clones containing appropriate PCR products was used for the sequencing reaction. In each case, at least 3 of the plasmid clones were sequenced.

FISH Analysis

Interphase FISH was performed according to standard procedure using cosmid probe N96A6 for the *SNF5* gene [8].

Results

Cytogenetic Analysis

To clarify the alterations of 22q where the *SNF5*gene resides, we first reviewed the archives of karyotypes from 168 patients (121 CMLs, 10 AMLs, 5 MDS, 13 B lymphoblastic leukemia/lymphomas, 11 plasma cell myelomas, 6 diffuse large B-cell lymphomas, 2 peripheral T-cell lymphomas, NOS) that had chromosome 22 abnormalities in

Table 3. Abnormalities of chromosome 22 in hematological neoplasms

t(9;22)(q34;q11.2)	117 CMLs, *BCR-ABL1* positive 10 B lymphoblastic leukemia/lymphomas with t(9;22)(q34;q11.2);*BCR-ABL1* 1 refractory cytopenia with multilineage dysplasia 1 DLBCL
-22	6 AMLs with myelodysplasia-related changes 1 AML with t(8;21)(q22;q22);*RUNX1-RUNX1T1* 1 AML with maturation 3 RAEB-2 3 B lymphoblastic leukemia/lymphomas, NOS 1 T lymphoblastic leukemia/lymphoma 7 plasma cell myelomas 3 DLBCLs 1 Burkitt lymphoma 1 anaplastic large cell lymphoma
+22	3 AMLs with myelodysplasia-related changes 1 T lymphoblastic leukemia/lymphoma 2 plasma cell myelomas 1 DLBCL 2 angioimmunoblastic T-cell lymphomas 1 peripheral T-cell lymphoma, NOS
22q-	1 B lymphoblastic leukemia/lymphoma, NOS
22q+	1 DLBCL, 1 B lymphoblastic leukemia/lymphoma, NOS
+22q-	1 lymphoplasmacytic lymphoma
-22,-22	1 plasma cell myeloma 1 DLBCL
-22,22q-	1 B lymphoblastic leukemia/lymphoma, NOS 1 DLBCL
-22,del(22)(q11.2 q13)	1 RAEB-2
-22,del(22)(q13)	1 AML with myelodysplasia-related changes
der(21;22)(q10;q10)	1 plasma cell myeloma
der(22)t(1;22)(q12~21;p13)	1 plasma cell myeloma
del(22)(q13.?1)	1 DLBCL
t(2;9;22)(p21;q34;q11.2)	1 CML, *BCR-ABL1*-positive
t(7;9;22)(q22;q34;q11.2)	1 CML, *BCR-ABL1*-positive
t(10;9;22)(q22;q34;q11.2)	1 CML, *BCR-ABL1*-positive
t(9;22)(q34;q11.2),+der(22)t(9;22)	2 CMLs, *BCR-ABL1*-positive

our institute. Since the majority of the karyotypes were obtained from CML, we next analyzed karyotypes in an additional 115 patients with different types of hematological malignancies (3 CMLs, 22 AMLs, 23 MDS, 10 lymphoblastic leukemia/lymphomas, 21 plasma cell myelomas, 10 diffuse large B-cell lymphomas, 9 follicular lymphomas, 2 lymphoplasmacytic lymphomas, 2 Burkitt lymphomas, 6 adult T-cell leukemia/lymphomas, 3 peripheral T-cell lymphomas, 2 angioimmunoblastic T-cell lymphomas, 2 anaplastic large cell lymphomas) irrespective of information about chromosome abnormalities. As a total, karyotypes were reviewed in the 283 patients with

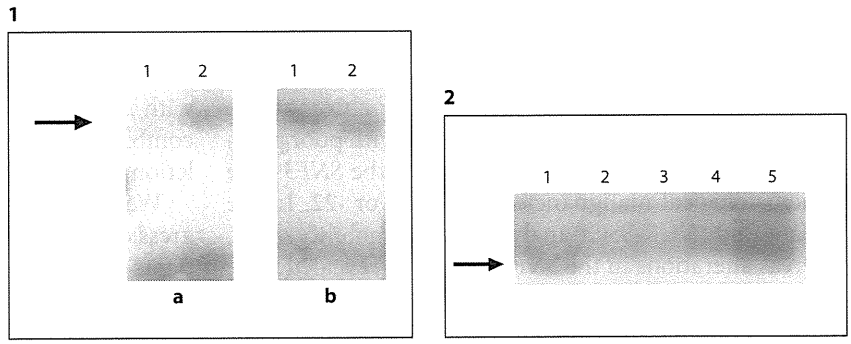

Fig. 1. LOH on 22q in plasma cell myeloma. The upper allele was deleted at the *D22S1169* locus in MM1 (**a**), while both alleles were retained in MM2 (**b**). 1 = Myeloma; 2 = lymphocyte.

Fig. 2. PCR-SSCP analysis was performed in hematological neoplasms. Aberrant bands were detected in lanes 1 and 5. Lane 1 = CML4; lane 2 = CML5; lane 3 = CML6; lane 4 = CML7; lane 5 = CML8. Arrow indicates aberrant bands.

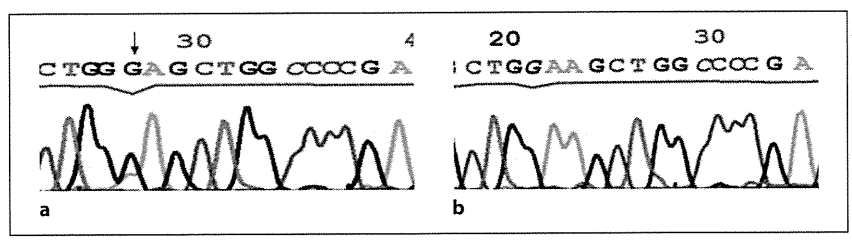

Fig. 3. Sequence analysis was performed in the *SNF5* gene. **a** Nucleotide change (A to G) was found 41 bp upstream from exon 9 (CML4). **b** Control.

Color version available online

hematological neoplasms as described in 'Patients and methods' ('Cytogenetic analysis'). Alterations of chromosome 22 were found in 184 of the 283 neoplasms (table 3). The most frequent alterations were t(9;22)(q34;q11.2) found in 119 CMLs and 10 B lymphoblastic leukemia/lymphomas. Monosomy 22 or 22q- was observed in 36 patients (table 3).

LOH Analysis

Although cytogenetic analysis showed 22q- or -22 in 8 of the 32 plasma cell myelomas (table 3), it is sometimes difficult to obtain metaphase from myeloma cells. Therefore we collected 21 paired samples of myeloma cells and peripheral lymphocytes from the same individuals without chromosome 22 abnormalities. We screened for LOH with 5 microsatellite markers spanning chromosome 22 in the 21 patients with plasma cell myeloma. Allelic loss at *D22S1169*, distal to *SNF5*, was detected in 1 of the 21 plasma cell myelomas (5%; MM1, fig. 1a). No allelic loss was observed at the other markers in any of the 21 patients.

PCR-SSCP Analysis and Sequencing

Since the 8 hematological malignancies had -22 or 22q- and of which DNA was available, we examined mutations that may cause inactivation of the *SNF5* gene on the remaining allele. We also analyzed mutations in 8 CMLs in BC since a previous study indicated that deletion at the t(9;22) breakpoint was associated with poor prognosis in CML, and loss of *SNF5* was acquired during the course of the disease [12, 13]. PCR-SSCP analysis was performed on all of the coding exons in the 16 hematological malignancies ('Patients and methods', 'Extraction of DNA'). Clinical information was available for these 16 patients as shown in table 1. PCR-SSCP analysis covering exon 9 of the *SNF5* gene showed mobility shifts in 2 CML samples (fig. 2). However, sequence analysis showed known polymorphisms in intron 8 (41 bp upstream from exon 9; fig. 3) [12].

FISH Analysis

FISH analysis was performed in 1 case of MDS (RAEB-2) with 44,XX, -5, -18, -20, -22, ?del (22)(q11.2 q13), +mar1, +mar2, min. Although no normal chromosome 22 was observed, FISH analysis revealed that both alleles of the *SNF5* gene were retained in this case (data not shown).

Discussion

Recent studies have shown that the genes associated with chromatin remodeling were altered in acute promyelocytic leukemia with t(15;17)(q22;q12), *PML-RARA* and acute leukemia with 11q23 abnormalities [18, 19]. The *SNF5* gene encodes a member of the SW1/SNF chromatin remodeling complex. The gene is inactivated by

mutation on one allele accompanied with loss of the 2nd allele in RT. Previous studies have indicated that the gene is deleted in CML and that deletions of chromosome arms 9q and/or 22q have been associated with poor prognosis [12, 13]. We analyzed alterations of the *SNF5* gene in hematological malignancies with 22q- or -22. In the present study, PCR-SSCP analysis showed mobility shifts, whereas alterations in the *SNF5* gene were revealed to be known polymorphisms [12]. These results suggest that the alterations of the *SNF5* gene on the remaining allele are rare in hematological malignancies. Another possibility of inactivation is that one allele is methylated and not expressed, and the 2nd allele is lost. However, methylation of the *SNF5* gene was not observed in RT [20]. Alternatively, haploinsufficiency of the *SNF5* gene may contribute to the development of these neoplasms. This has been shown in familial thrombocytopenia disorder with the loss of one *AML1* allele associated with an increased proclivity to develop AML [21].

In contrast to the initial report, a subsequent study showed that hSNF5 inactivation was mainly associated with homozygous deletions and mitotic recombination in RT [22]. Our cytogenetic analysis showed possible homozygous deletions encompassing the *SNF5* gene in several neoplasms. FISH analysis was performed in one RAEB-2 with -22, ?del (22)(q11.2 q13), marker chromosomes, whereas it failed to show homozygous deletions of the gene in this case.

Deletions of 22q have been reported in a subset of plasma cell myelomas [23]. The relatively high incidence of 22q- or -22 found in our myeloma patients was probably affected by selection bias as mentioned above. The current study showed LOH on 22q in 1 of the 21 myelomas (5%). Since cytogenetic analysis did not show either 22q deletions or monosomy of chromosome 22 in the case with LOH on 22q, our findings suggest that mitotic recombination or a small cytogenetically undetectable deletion is the mechanism that resulted in LOH on 22q.

We previously examined 22q for allelic loss in the progression of CML using microsatellite markers in 30 patients who progressed from chronic phase to BC. We detected LOH on 22q in 2 of 18 informative patients with CML BC (11%) [3]. We also reported allelotype analysis in the progression of MDS to AML, and found that 1 of the 20 samples (5%) had LOH on 22q [4]. These findings suggest that LOH on 22q was not frequent, but was involved in a substantial proportion of these hematological neoplasms.

In summary, this study showed that deletion or loss of 22q is found in a subset of hematological neoplasms, and that alterations of the *SNF5* gene are rare in hematological malignancies with chromosome 22 abnormalities. Another gene may be the target for alterations on 22q. Identification and characterization of the affected gene(s) from 22q in hematological neoplasms will help elucidate the genesis of disease progression and novel therapeutic strategies.

Acknowledgements

This work was supported in part by a grant-in-aid from the Ministry of Education, Culture, Sports, Science and Technology of Japan. The chromosome-specific gene library LL22NC03 was constructed at the Biomedical Sciences Division, Lawrence Livermore National Laboratory Gene Library Project, sponsored by the U.S. Department of Energy. Cosmid N96A6 was kindly provided by Dr. Olivier Delattre (Institut Curie, Paris, France). We thank Mari Ohwashi for her technical assistance.

References

1 Weinberg RA: Tumor suppressor genes. Science 1991;254:1138–1146.
2 Knudson AG: Mutation and cancer: statistical study of retinoblastoma. Proc Natl Acad Sci USA 1971;68:820–823.
3 Mori N, Morosetti R, Lee S, Spira S, Ben-Yehuda D, Schiller G, Landolfi R, Mizoguchi H, Koeffler HP: Allelotype analysis in the evolution of chronic myelocytic leukemia. Blood 1997;90:2010–2014.
4 Mori N, Morosetti R, Hoflehner E, Lubbert M, Mizoguchi H, Koeffler HP: Allelic loss in the progression of myelodysplastic syndrome. Cancer Res 2000;60:3039–3042.
5 Kalpana GV, Marmon S, Wang W, Crabtree GR, Goff SP: Binding and stimulation of HIV-1 integrase by a human homolog of yeast transcription factor SNF5. Science 1994;266:2002–2006.
6 Muchardt C, Sardet C, Bourachot B, Onufryk C, Yaniv M: A human protein with homology to *Saccharomyces cerevisiae* SNF5 interacts with the potential helicase hbrm. Nucleic Acids Res 1995;23:1127–1132.
7 Wang W, Xue Y, Zhou S, Kuo A, Cairns BR, Crabtree GR: Diversity and specialization of mammalian SWI/SNF complexes. Genes Dev 1996;10:2117–2130.
8 Versteege I, Sevenet N, Lange J, Rousseau-Merck M-F, Ambros P, Handgretinger R, Aurias A, Delattre O: Truncating mutations of hSNF5/INI1 in aggressive paediatric cancer. Nature 1998;394:203–206.
9 Sevenet N, Lellouch-Tubiana A, Schofield D, Hoang-Xuan K, Gessler M, Birnbaum D, Delattre O: Spectrum of hSNF5/INI1 somatic mutations in human cancer and genotype-phenotype correlations. Hum Mol Genet 1999;8:2359–2368.
10 Roberts CW, Galusha SA, McMenamin ME, Fletcher CDM, Orkin SH: Haploinsufficiency of Snf5 (integrase interactor 1) predisposes to malignant rhabdoid tumors in mice. Proc Natl Acad Sci USA 2000;97:13796–13800.

11 Roberts CW, Leroux MM, Fleming MD, Orkin SH: Highly penetrant, rapid tumorigenesis through conditional inversion of the tumor suppressor gene Snf5. Cancer Cell 2002; 2:415–425.
12 Grand F, Kulkarni S, Chase A, Goldman JM, Gordon M, Cross NCP: Frequent deletion of hSNF5/INI1, a component of the SWI/SNF complex, in chronic myeloid leukemia. Cancer Res 1999;59:3870–3874.
13 Sinclair PB, Nacheva EP, Leversha M, Telford N, Chang J, Reid A, Bench A, Champion K, Huntly B, Green AR: Large deletions at the t(9;22) breakpoint are common and may identify a poor-prognosis subgroup of patients with chronic myeloid leukemia. Blood 2000;95:738–744.
14 Yuge M, Nagai H, Uchida T, Murate T, Hayashi Y, Hotta T, Saito H, Kinoshita T: hSNF5/INI1 gene mutations in lymphoid malignancy. Cancer Genet Cytogenet 2000; 122:37–42.
15 Su Y-C, Chen C-B, Chang Y-T, Tung Y-T, Li D-K: hSNF5/INI1 mutation analysis in acute myeloid leukemia. Int J Hematol 2008;87: 172–175.
16 Litt M, Luty JA: A hypervariable microsatellite revealed by in vitro amplification of a dinucleotide repeat within the cardiac muscle actin gene. Am J Hum Genet 1989;44:397–401.
17 Mori N, Wada M, Yokota J, Terada M, Okada M, Teramura M, Masuda M, Hoshino S, Motoji T, Oshimi K, Mizoguchi H: Mutations of the p53 tumour suppressor gene in haematologic neoplasms. Br J Haematol 1992;81:235–240.
18 Redner RL, Wang JX, Liu JM: Chromatin remodeling and leukemia: new therapeutic paradigms. Blood 1999;94:417–428.
19 Müller C, Leutz A: Chromatin remodeling in development and differentiation. Curr Opin Genet Dev 2001;11:167–174.
20 Zhang F, Tan L, Wainwright LM, Bartolomei MS, Biegel JA: No evidence for hypermethylation of the hSNF5/INI promoter in pediatric rhabdoid tumors. Genes Chromosom Cancer 2002;34:398–504.
21 Song W-J, Sullivan MG, Legare RD, Hutchings S, Tan X, Kufrin D, Ratajczak J, Resende IC, Haworth C, Hock R, Loh M, Felix C, Roy D-C, Busque L, Kurnit D, Willman C, Gewirtz AM, Speck NA, Bushweller JH, Li FP, Gardiner K, Poncz M, Maris JM, Gilliland DG: Haploinsufficiency of CBFA2 causes familial thrombocytopenia with propensity to develop acute myelogenous leukaemia. Nature Genet 1999;23:166–175.
22 Rousseau-Merck M-F, Versteege I, Legrand I, Couturier J, Mairal A, Delattre O, Aurias A: hSNF5/INI1 inactivation is mainly associated with homozygous deletions and mitotic recombinations in rhabdoid tumors. Cancer Res 1999;59:3152–3156.
23 Smadja NV, Bastard C, Brigaudeau C, Leroux D, Fruchart C: Hypodiploidy is a major prognostic factor in multiple myeloma. Blood 2001;98:2229–2238.

3．骨髄異形成症候群（MDS）関連遺伝子

牧　和宏[1]・三谷　絹子[2]
Maki Kazuhiro Mitani Kinuko

獨協医科大学 内科学（血液・腫瘍） [1]講師 [2]教授

Summary　骨髄異形成症候群は疾患群であり，様々な遺伝子が骨髄異形成症候群の発症に関与していると考えられるが，最近まで病態の解明は進んでいなかった。最近になり，相次いでTET2，CBL，ASXL1，EZH2などの骨髄異形成症候群に関連した遺伝子が見いだされている。これらはいずれもSNPアレイを用いた解析により同定されており，SNPアレイは疾患の原因遺伝子検索の強力なツールである。今後も骨髄異形性症候群のさらなる病態解明が予想される。また，病態解明により，骨髄異形性症候群に対する新規治療の開発も期待される。

はじめに

骨髄異形成症候群（Myelodysplastic syndrome：MDS）は，無効造血による血球減少と急性骨髄性白血病（Acute myelogenous leukemia：AML）への進展を特徴とする造血幹細胞レベルの腫瘍性疾患である。MDSは疾患群であり，様々な遺伝子がMDSの発症に関与していると考えられるが，疾患の不均一性や動物モデル作製が困難であることなどの理由でその病態の解明は進んでいなかった。最近になり，相次いでMDSに関連した遺伝子が見いだされており[1]（**表1**），本稿ではこれらのMDSについて概説する。

1．5q－症候群関連遺伝子

MDSに高頻度に見られる染色体異常としては，5番染色体長腕欠失（5q－：5q－症候群），7番染色体欠失（-7）/7番染色体長腕欠失（7q－），20番染色体長腕欠失（20q－）などがあるが，その中でも5q－症候群は，そのMDS関連遺伝子についての解析が最も進んでいる。上記のように染色体の部分欠失と疾患との関連が疑われる場合には，多数例において欠損部位を解析することで，責任遺伝子が存在すると考えられる共通欠損領域を絞り込むことができる。5q－症候群においては，5q31.1（近位共通欠損領域）と5q33.1（遠位共通欠損領域）に2つの共通欠損領域があることがわ

MDS（Myelodysplastic syndrome；骨髄異形成症候群）　AML（Acute myelogenous leukemia；急性骨髄性白血病）

表1　骨髄異形成症候群関連遺伝子

遺伝子	骨髄腫陽性疾患				
	MDS	CMML	JMML	MPN	AML
TET2	3＋	3＋	−	2＋	3＋
RUNX1	2＋	3＋		1＋	2＋
NRAS/KRAS	2＋	3＋	3＋	rare	2＋
ASXL1	2＋	3＋		2＋	2＋
TP53	2＋	−			2＋
CBL	2＋	3＋	2＋	1＋	1＋
JAK2	1＋	1＋		3＋	1＋

（文献1より改変）

かっており，遠位共通欠損領域には40個の遺伝子が存在する。そのうちの一つであるRPS14遺伝子は，RNA干渉（**RNAi**）を用いたスクリーニングにより見いだされた5q－症候群関連遺伝子である[2]。RPS14はリボゾームRNAの40Sサブユニットの構成蛋白をコードする遺伝子であるが，ヒトCD34陽性造血前駆細胞においてRNAiによりRPS14蛋白をノックダウンすることによって，5q－症候群と同様の表現型（赤芽球系細胞の著明な分化抑制）が再現され，逆に患者骨髄細胞にRPS14を強制発現させることにより赤芽球系細胞の分化が回復されることが示されている。これらの結果より，RPS14遺伝子は5q－症候群の原因遺伝子の一つと考えられている。他のリボゾーム関連蛋白であるRPS17，RPS19，RPS24が赤芽球系の著名な低形成を呈する先天性の赤芽球癆（Diamond-Blackfan症候群）の原因遺伝子として同定されていることも，リボゾームと赤血球造血の関連を考える上で興味深い。SPARC遺伝子も5q－症候群関連遺伝子として同定された遺伝子であるが，この遺伝子は5q－症候群患者の赤芽球をレナリドミド処理した際に発現が回復する遺伝子として見いだされている[3]。レナリドミド（レブラミド®）はサリドマイド誘導体として開発された薬であるが，MDSの中でも特に5q－症候群に対する有効性が高く，日本でも5q－症候群（および多発性骨髄腫）の治療薬として先頃承認されている。SPARCは抗血管形成作用を有するほか，癌抑制因子でもあると考えられており，AMLを含む多くの癌においてSPARC遺伝子の発現低下が認められている。SPARCもRPS14と同様に遠位共通欠損領域に位置する遺伝子であり，5q－症候群の原因遺伝子の一つと考えられている。

一方，近位共通欠損領域に位置する遺伝子の中では，CTNNA1遺伝子（αカテニン遺伝子），EGR1遺伝子，HSPA9遺伝子が5q－症候群の関連遺伝子の候補として同定されている。これらの遺伝子はいずれも癌抑制遺伝子であると考えられている。CTNNA1遺伝子は，5q－症候群患者の白血病幹細胞分画（$CD34^+CD38^-CD123^+Lin^-$）において正常細胞と比較し，著明に発現が低下している遺伝子として同定された[4]。5q－を有する細胞株HL-60では，CTNNA1遺伝子の正常アレルのエピジェネティックな機序による不活化が観察され，CTNNA1遺伝子の強制発現によりHL-60細胞の増殖抑制・アポトーシス誘導が認められる。EGR-1遺伝子はWT-1ファミリーに属する転写因子でp53による細胞分裂制御のゲートキーパーと考えられているが，EGR-1のヘテロノックアウトマウスに抗癌剤N-ethyl-nitrosourea（**ENU**）を投与するとT細胞リンパ腫や骨髄増殖症候群の発症が認められた。特に骨髄増殖症候群では白血球増加および無効造血による貧血・血小板を呈することから，EGR-1のhaploinnsufficiencyと5q－症候群との関連が示唆される。

RNAi（RNA干渉）　ENU（N-ethyl-nitrosourea）